

GRISEOFULVIN POTENTIATES ANTITUMORIGENESIS EFFECTS OF NOCODAZOLE THROUGH INDUCTION OF APOPTOSIS AND G2/M CELL CYCLE ARREST IN HUMAN COLORECTAL CANCER CELLS

Yuan-Soon Ho^{1*}, Jiing-Shium DUH¹, Jjiang-Huei JENG², Ying-Jan WANG³, Yu-Chih LIANG⁴, Chien-Huang LIN¹, Chia-Jen TSENG¹, Cheng-Fei YU¹, Rong-Jane CHEN¹ and Jen-Kun LIN⁴

¹Institute of Biomedical Technology, Taipei Medical College, Taipei, Taiwan

²School of Dentistry, College of Medicine, National Taiwan University, Taipei, Taiwan

³Department of Environmental and Occupational Health, National Cheng Kung University Medical College, Taipei, Taiwan

⁴Institute of Biochemistry, College of Medicine, National Taiwan University, Taipei, Taiwan

In this study, we demonstrate that apoptosis and G2/M cell cycle arrest were easily induced by treatment with the oral antifungal agent, griseofulvin (GF). The mechanisms of GF-induced G2/M arrest were characterized as (a) induction of abnormal mitotic spindle formation, (b) elevation of cyclin B1/cdc2 kinase activity and (c) down-regulation of myt-1 protein expression. On the other hand, caspase 3 activation, Bcl-2 hyperphosphorylation and inhibition of the normal function of Bcl-2 associated with Bax were demonstrated to be the mechanisms of GF-induced apoptosis. DNA fragmentation and flow cytometry analyses demonstrated that combined treatment of GF with the cancer chemotherapeutic agent, nocodazole (ND), strongly potentiates the apoptotic effect and arrest of the G2/M cell cycle in 5 types of human cancer cells, but not in normal human keratinocytes (#76 KhGH). The combined treatment of GF and ND triggered the polymerization of purified tubulin in HT 29 but not in #76 KhGH cells. To further confirm these observations, the therapeutic efficacy was further examined *in vivo* by treating athymic mice bearing COLO 205 tumor xenografts, with GF (50 mg/kg), ND (5 mg/kg) or GF + ND. Combined treatment of GF and ND significantly enhanced the effect of ND, and led to cessation of tumor growth. These results suggest that chemotherapeutic agents (such as ND) administered in the presence of GF might provide a novel therapy for colorectal cancer.

© 2001 Wiley-Liss, Inc.

Key words: Griseofulvin; Bcl-2; apoptosis; microtubule; G2/M arrest.

Apoptosis is an active and gene-directed form of cell death with well-characterized morphological and biochemical features.¹ It has been indicated that the Bcl-2 family is involved in the regulation of apoptosis.^{2–4} Some proteins within this family, including Bcl-2 and Bcl-xL, have been shown to inhibit apoptosis triggered by a variety of stress stimuli.⁵ Bcl-2 and related antiapoptotic proteins have been shown to dimerize with a proapoptotic molecule, Bax, and modulate the sensitivity of a cell to apoptosis,⁶ which may constitute a barrier to the success of cancer therapy. Initiation of apoptosis appears to be a common mechanism of many cytotoxic agents used in cancer chemotherapy. Treatment of tumor cells with antitumor agents usually results in the breakdown of the cell cycle machinery. Agents with diverse primary targets and binding sites, including topoisomerase II inhibitors, DNA alkylating agents, antibiotics and folate antagonists, initiate pathways of gene and protein expression leading to apoptosis.⁷ Recently, microtubules have been demonstrated to be the new target of many widely used cancer chemotherapeutic agents including taxanes, paclitaxel, cryptophycins and docitaxel by causing specific loss of normal functions of cellular microtubules.^{8,9}

According to recent reports, microtubule-stabilizing agents such as paclitaxel and docetaxel¹⁰ and microtubule-disrupting drugs such as vincristine, vinblastine and colchicine have antimetabolic and apoptosis-inducing activity.¹¹ In these studies, human leukemic, breast cancer and prostate cancer cells exposed to paclitaxel expressed a phosphorylated form of Bcl-2 and underwent apoptosis, suggesting that phosphorylation of Bcl-2 may inhibit Bcl-2 function.¹⁰ In addition, phosphorylation of Bcl-2 appears to inhibit its

binding to Bax, since less Bax was observed in an immunocomplex with Bcl-2 in taxol-treated cancer cells.¹² Other studies have indicated that Bcl-2 phosphorylation is tightly associated with mitotic arrest, but is not a determinant of progression into apoptosis after mitotic arrest induced by antitubulin agents such as taxol and nocodazole (ND).^{13–15} The correlation of G2/M arrest and apoptosis was investigated in reports that demonstrated that activation of protein kinase A (or raf-1) due to microtubule damage is an important event in Bcl-2 (or Bcl-x_L) phosphorylation.^{10,16} How disruption of the microtubules can lead to cell death is only now being explored.

The ability of cancer chemotherapeutic agents to initiate apoptosis is an important determinant in their therapeutic response. Our previous results showed that the oral antifungal agent, ketoconazole, caused apoptosis in human cancer cell lines.¹⁷ The present work extends the previous study, and the data indicate that another antifungal agent, griseofulvin (GF), at micromolar concentrations, rapidly initiates apoptosis. The goal of this study was to increase our understanding of GF-induced apoptosis and G2/M cell cycle arrest and also to elucidate general mechanisms through which intracellular signals can mediate these responses.

MATERIAL AND METHODS

Cell lines and cell culture

The cell line HT 29 (HTB-38; American Type Culture Collection [ATCC], Rockville, MD) was isolated from a moderately well differentiated grade II human colon adenocarcinoma. The cell line COLO 205 (CCL-222; ATCC) was developed from a poorly differentiated human colon adenocarcinoma. The cell line #76 KhGH (CRL 8858; ATCC) was composed of keratinocytes derived from normal human epidermis. Hep 3B cells (HB 8064; ATCC) were derived from a human hepatocellular carcinoma line. The cell line Hep G2 (HB 8065; ATCC) was also derived from a human hepatocellular carcinoma line. Cell lines were grown at 37°C in a 5% CO₂ atmosphere in Eagle's minimal essential me-

Abbreviations: DMSO, dimethyl sulfoxide; EP, etoposide; FCS, fetal calf serum; GF, griseofulvin; ND, nocodazole; PARP, poly-(ADP ribose) polymerase

Grant sponsor: National Science Council; Grant number: NSC 88-2621-B-038-002-Z; Grant sponsor: National Health Research Institute; Grant number: DOH 86-HR-403.

*Correspondence to: Institute of Biomedical Technology, Taipei Medical University, No. 250, Wu-Hsing Street, Taipei, Taiwan. Fax: (886)2-2739-3422. E-mail: hoyuansn@tmc.edu.tw

Received 23 May 2000; Revised 1 September 2000; Accepted 5 September 2000

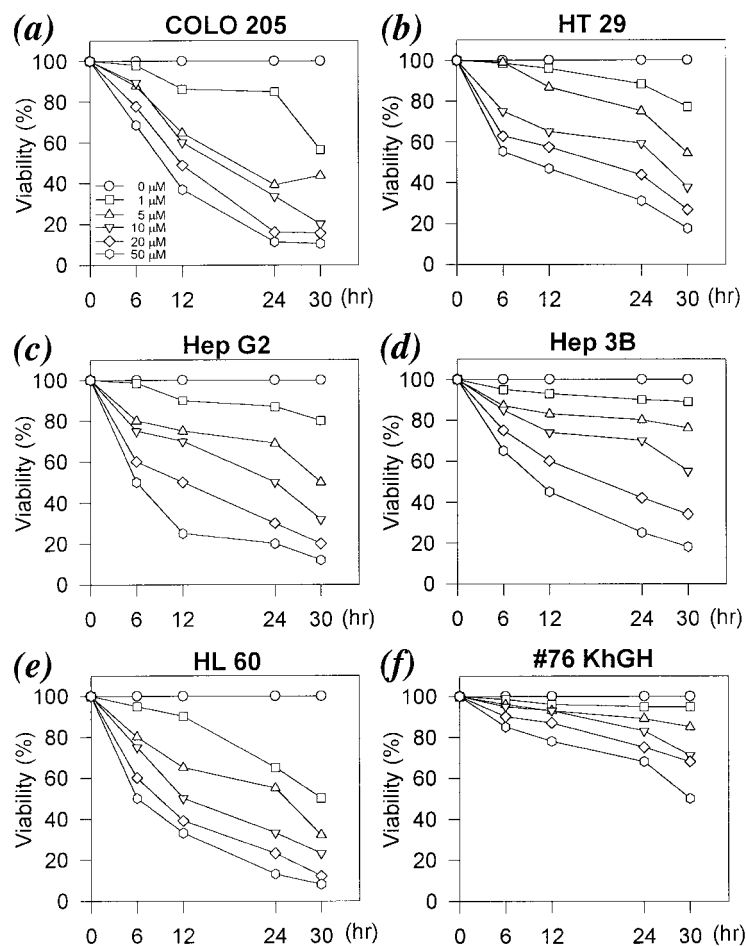


FIGURE 1 – Viability of human normal and cancer cells treated with various doses of griseofulvin (GF). (a) COLO 205, (b) HT 29, (c) Hep G2, (d) Hep 3B, (e) HL 60 and (f) #76 KhGH cells were treated with various concentrations of GF (0 to 50 μM). The cell viability was measured at the indicated time points after exposure to GF. Results are the means of three independent experiments.

dium (for Hep G2, and Hep 3B cells), RPMI 1640 (for COLO 205, HL 60 and HT-29 cells), supplemented with 10% fetal calf serum (FCS), 50 $\mu\text{g}/\text{ml}$ gentamycin and 0.3 mg/ml glutamine. A 3:1 mixture of Ham's F12 medium and Dulbecco's modified Eagle's medium (for #76 KhGH cells) supplemented with 10% FCS, 40 ng/ml hydrocortisone, 0.01 mg/ml cholera toxin, 0.005 mg/ml insulin and 10 ng/ml epidermal growth factor.

Determination of cell viability

Cell viability was determined at indicated times based on the Trypan blue exclusion method as described previously.¹⁸ The viability percentage was calculated based on the percentage of unstained cells.

Cell synchronization, drug treatment and flow cytometry analysis

At 72 hr after plating of cells, cells were synchronized with medium containing 8 mM glutamine and 0.04% FCS for 24 hr. After synchronization, the cells were stimulated by the addition of medium containing 10% serum. The stock solutions of drugs (dissolved in dimethyl sulfoxide [DMSO]) were diluted with serum-free medium to yield final concentrations as indicated in the text. Cells were incubated with 50 $\mu\text{g}/\text{ml}$ propidium iodide (Sigma, St. Louis, MO), and DNA content was measured using a FACScan laser flow cytometer analysis system (Becton Dickinson, San Jose, CA); 15,000 events were analyzed for each sample.

Indirect immunofluorescence staining

The technique of immunofluorescence staining has been described previously.¹⁸

Cell protein extraction and immunoprecipitation

Treated or untreated cells were collected for protein extraction as described previously.¹⁹ Equal amounts of protein were immunoprecipitated with saturating amounts of anti-cyclin B1 antibody. Immunoprecipitates were washed 5 times with extraction buffer and once with phosphate-buffered saline. The pellet was then resuspended in sample buffer (50 mM Tris, pH 6.8; 100 mM dithiothreitol; 2% sodium dodecyl sulfate [SDS]; 0.1% bromophenol blue; 10% glycerol) and incubated for 10 min at 90°C before electrophoresis to release the proteins from the beads.

Western blot analysis

Treated and untreated cells were lysed in freshly prepared extraction buffer (10 mM Tris-HCl, pH 7, 140 mM sodium chloride, 3 mM magnesium chloride, 0.5% [v/v] NP-40, 2 mM phenylmethylsulfonyl fluoride [PMSF], 1% [w/v] aprotinin and 5 mM dithiothreitol) for 20 min on ice. Proteins (50 $\mu\text{g}/\text{lane}$) resolved on 12.5% [w/v] SDS-polyacrylamide gel, blotted, and analyzed using specific antibodies, including polyclonal rabbit anti-human Bax antisera (Transduction Laboratories, Lexington, KY) and mouse monoclonal antibodies against lamin A (JOL4, Serotec Co., Oxford, England), myt-1 (Santa Cruz Biotechnologies, Santa Cruz, CA), Bcl-2, PARP, cyclin B1 and cdc2 kinase (Transduction

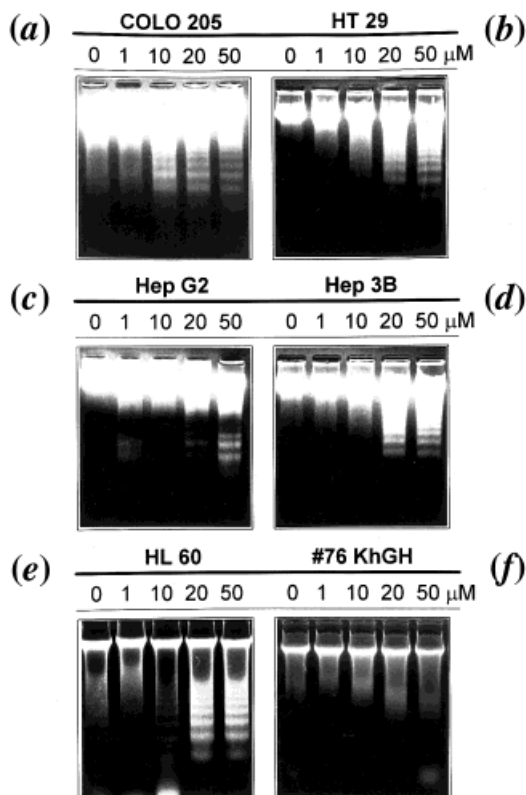


FIGURE 2 – Induction of apoptosis by griseofulvin (GF) in human cancer cells. (a) COLO 205, (b) HT 29, (c) Hep G2, (d) Hep 3B, (e) HL 60 and (f) #76 KhGH cells were treated with various doses of GF (0–50 μM) for 24 hr. DNA fragmentation was detected by 1.75% agarose gel electrophoresis.

Laboratories). Immunoreactive bands were visualized by incubating with the colorigenic substrates, nitro blue tetrazolium and 5-bromo-4-chloro-3-indolyl-phosphate (NBT/BCIP) (Sigma).

Immunoprecipitation and Cdc2 kinase activity assay

The protein lysate (100 μg in 0.5 ml of extraction buffer) was immunoprecipitated with 5 μg monoclonal anti-cyclin B1 antibody. The immuno-complexes were washed 3 times with the lysis buffer and once with kinase buffer containing 50 mM Tris-HCl (pH 7.4), 10 mM MgCl_2 , and 1 mM dithiothreitol. The beads were incubated with 50 μl of kinase reaction mixture containing 50 mM Tris-HCl (pH 7.4), 10 mM MgCl_2 , 1 mM dithiothreitol, 10 μM ATP, 5 μCi of [γ - ^{32}P] ATP, and 0.5 mg/ml of histone H1 for 15 min. The reaction was terminated by the addition of 20 μl of 4 \times Laemmli's sample buffer and boiling for 5 min. The ^{32}P -phosphorylated histone H1 was separated by 0.1% SDS, 10% polyacrylamide gel and determined by autoradiography using Kodak X-Omat film.

Tubulin polymerization assay

This assay has been described elsewhere.²⁰ Cells were lysed with 100 μl of hypotonic buffer (1 mM MgCl_2 , 2 mM EGTA, 0.5% Nonidet P-40, 2 mM PMSF, 200 unit/ml aprotinin, 100 $\mu\text{g}/\text{ml}$ soybean trypsin inhibitor, 50 mM ϵ -amino caproic acid, 1 mM benzamidine and 20 mM Tris-HCl, pH 6.8) at 37°C for 5 min in the dark. The lysate was treated without or with GF (20 μM) and/or ND (0.25 μM). The lysates were transferred to Eppendorf tubes, and each well was rinsed with 100 μl of hypotonic buffer. Following a brief but vigorous vortexing, the samples were centrifuged at 14,000 rpm for 10 min at room temperature. The 200- μl supernatants containing soluble (cytosolic) tubulin were trans-

ferred to another Eppendorf tube separating them from the pellets containing polymerized (cytoskeletal) tubulin. The pellets were resuspended in 200 μl of hypotonic buffer.

The cytosolic and cytoskeletal fractions were each mixed with 70 μl of 4 \times SDS-polyacrylamide gel electrophoresis sample buffer (45% glycerol, 20% β -mercaptoethanol, 9.2% SDS, 0.04% bromophenol blue and 0.3 M Tris-HCl, pH 6.8) and heated at 95°C for 5 min. Twenty microliters of each sample was analyzed by immunoblotting, and was quantitated by densitometry. The percentage of polymerized tubulin was determined by dividing the densitometry value of polymerized tubulin by the total tubulin content (the sum of the densitometry values of soluble and polymerized tubulin).

Analysis of DNA fragmentation

Apoptosis was determined by DNA laddering and morphological criteria as described previously.²¹

Treatment of COLO 205-derived xenografts in vivo

COLO 205 cells (5×10^6) in 0.2 ml PBS were injected subcutaneously between the scapulae of each nude mouse (purchased from National Science Council animal center, Taipei). After transplantation, tumor size was measured using calipers and the tumor volume was estimated according to the following formula: tumor volume (mm^3) = $L \times W^2/2$, where L is the length and W is the width.²² Once tumors reached a mean size of 400 mm^3 , animals received either intraperitoneal injections of DMSO (25 μl), ND (5 mg/kg), GF (50 mg/kg), a combination of GF and ND or saline (as a control group) 3 times per week for 6 weeks.

RESULTS

GF induces apoptosis and G2/M cell cycle arrest in human cancer cells

In this study, human cancer cells, including colon adenocarcinoma cells (COLO 205 and HT 29), hepatoma cells (Hep G2 and Hep 3B) and leukemia cells (HL 60), and normal keratinocytes (#76 KhGH), were treated with various concentrations (0 to 50 μM) of GF. The minimal dose of GF that induced cytotoxicity in human cancer cells was 1 μM (Fig. 1). As described previously,²³ apoptosis is characterized by specific changes including DNA fragmentation and the presence of a sub-diploid peak following flow cytometry analysis. Figure 2 shows that GF induced DNA laddering in various cancer cells in a dose-dependent manner (0–50 μM). Our results from Figures 1 and 2 indicate that human cancer cell lines were more sensitive to GF than to normal human keratinocytes. The doses of GF that induced DNA fragmentation were found to be consistent with effective cytotoxic concentrations in various cell lines. Such results imply that the cytotoxic action of GF is due to its ability to induce apoptosis.

GF induces abnormal microtubule polymerization in HT 29 cells

The ability of GF to initiate DNA fragmentation was further evaluated with flow cytometry analysis. As shown in Figure 3a (left panel), a sub-diploid peak was easily observed in HT 29 cells at 24 hr after GF (10 μM) treatment. However, a higher dose of GF (>20 μM) was required to induce significant G2/M cell cycle arrest (Fig. 3a, left panel). The ability of GF to initiate microtubule changes coincident with mitotic arrest was illustrated by an immunofluorescence staining technique. A time-dependent experiment was conducted to determine whether GF-induced G2/M arrest is due to abnormal mitotic spindles. Before GF (20 μM) treatment, cells in the normal interphase were observed with bipolar mitotic spindles (Fig. 3a, arrowhead in middle panel). Treatment of cells with GF (20 μM) for 24 hr caused a marked presence of abnormal mitotic spindle formation with mono-, bi-, and tripolar spindles of varying lengths (Fig. 3a, right panel). By comparison, HT 29 cells were treated either with another microtubule damaging agent, ND (0–10 μM) (Fig. 3b, left panel) or the DNA topoisomerase II inhibitor, EP (0–10 μM) (Fig. 3c, left panel), to investigate

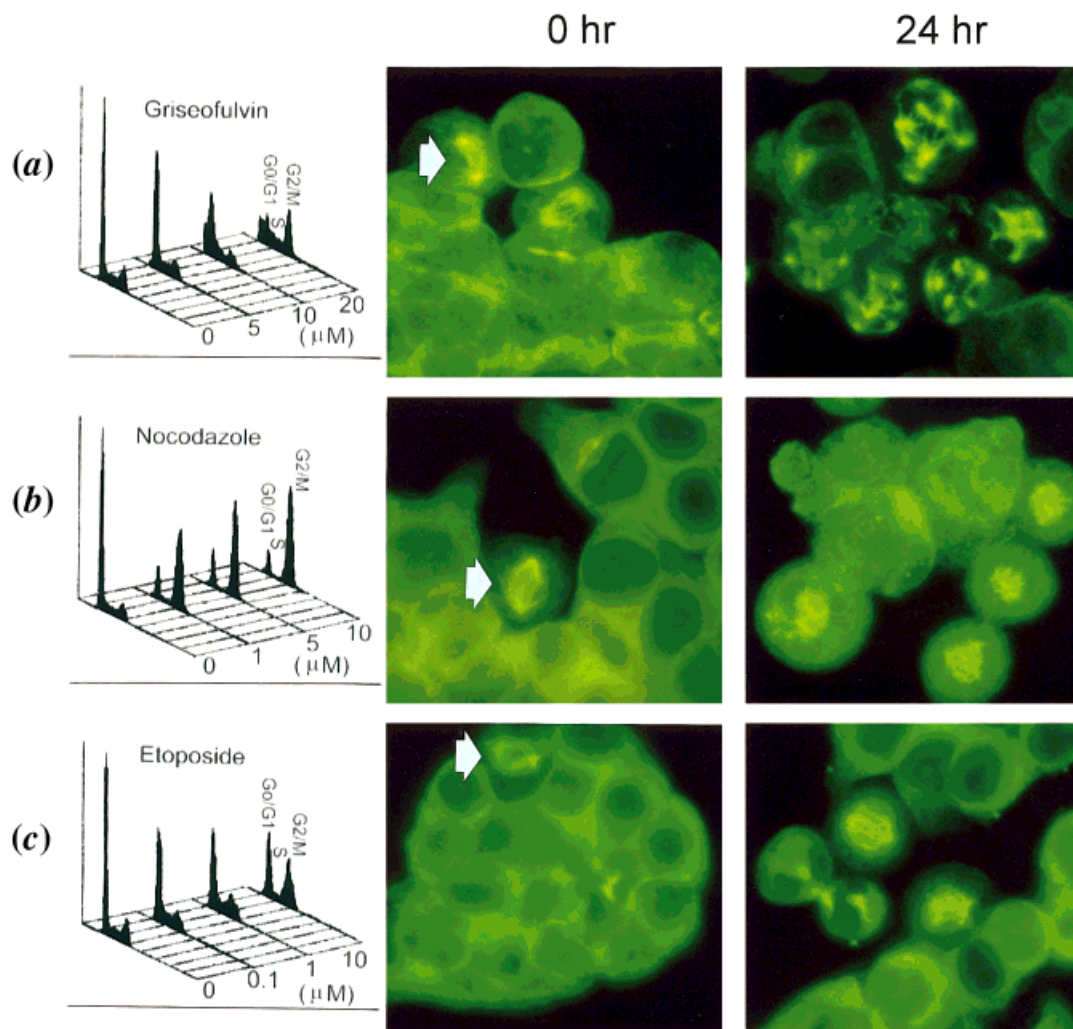


FIGURE 3—Comparison of G2/M cell cycle arrest and microtubules distortion in griseofulvin (GF)-, nocodazole (ND)- and etoposide (EP)-treated HT 29 cells. Left panel: HT 29 cells were treated with (a) GF (0–20 μM), (b) ND (0–10 μM) or (c) EP (0–10 μM) for 24 hr. G2/M cell cycle arrest was monitored by flow cytometry analysis. Right panel: Indirect immunofluorescence was also performed in HT 29 cells treated with (a) GF (20 μM), (b) ND (1 μM) or (c) EP (10 μM) for 24 hr. Middle panel: Cells without drug treatment serve as a control. The cells grown in cover slides were fixed, stained with anti- α -tubulin antibody and then detected by using indirect immunofluorescence staining technique as described in Material and Methods. Before treatment, cells in the normal interphase were observed with bipolar mitotic spindles (arrows).

whether GF- and ND-induced G2/M arrests were due to abnormal mitotic spindle formation. Our results indicate that abnormal microtubule spindles in HT 29 cells were observed in either GF (20 μM) or ND (1 μM) treatment (Fig. 3a,b, right panel), but not in EP (10 μM) treatment (Fig. 3c, right panel). Such results further confirm that GF-induced G2/M cell cycle arrest was due to abnormal microtubule polymerization.

Lower dose of GF induces apoptosis but not G2/M cell cycle arrest

To determine the minimal doses of GF and ND required for apoptosis in HT 29 cells, DNA fragmentation analysis was performed. Our results reveal that the minimal doses of GF and ND required for laddering were 10 μM (Fig. 2b lane 3 and Fig. 4a, lane 7) and 50 nM (data not shown), respectively. Importantly, DNA fragmentation was induced by combined treatment with both agents (Fig. 4a, lane 6). However, in such an extremely low dose, we found that combined treatment with GF and ND did not affect G2/M cell cycle arrest (Fig. 4b). Such observations demonstrate that the threshold for induction of apoptosis was lower than G2/M arrest in cells treated with GF.

In eukaryotic cells, execution of apoptosis depends on activation of a family of cysteine proteases, termed *caspases*.²⁴ Dose- and time-dependent experiments were performed to investigate the roles of caspase activation in GF-treated cells. The results show that caspase 3 was activated following 12 and 24 hr of GF (>5 μM) treatment (Fig. 5a,d). Poly (ADP-ribose) polymerase (PARP) has been identified as a substrate for caspase 3 cleavage.²⁵ The specific cleavage of PARP by activated caspase 3 results in the formation of an 85-kDa C-terminal fragment.²⁵ Our results show that the specific cleavage of PARP appeared 12–24 hr after GF (>5 μM) treatment (Fig. 5b,e). We further explored the possibility that GF treatment may also induce nuclear lamina protein degradation. Cleavage of lamin A was also observed at 18 hr later with a time progression that paralleled PARP degradation when cells were treated with GF (>10 μM) (Fig. 5c,f). These results demonstrate that GF initiates activation of the caspase cascade, consistent with the execution of a series of programmed events leading to apoptotic cell death.

Molecular mechanisms of GF-induced G2/M arrest

As shown in Figure 3a, a higher dose of GF (>20 μM) could induce G2/M arrest in human HT 29 cells. To further investigate

the molecular events in GF-induced G2/M arrest, HT 29 cells were synchronized at the G0/G1 phase by 0.04% serum starvation for 24 hr. After synchronization, the medium was replaced with the complete medium containing 10% FCS. The sub-population dur-

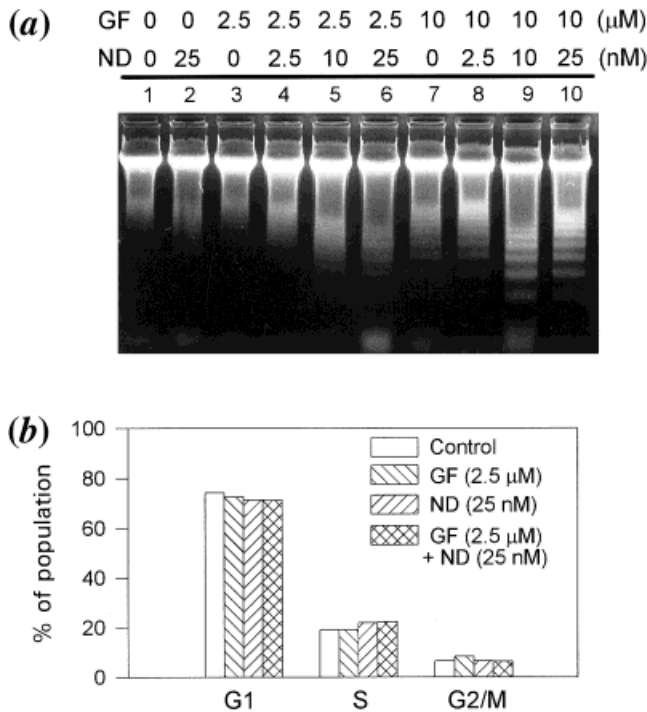


FIGURE 4 – Induction of apoptosis but not G2/M cell cycle arrest by combined treatment of low doses of griseofulvin (GF) and nocodazole (ND) in HT 29 cells. (a) HT 29 cells were treated with different doses of GF (0–10 μM), ND (0–25 nM) or GF + ND. DNA fragmentation was examined at 24 hr later. Cells in lane 1 received mock treatment as controls. (b) HT 29 cells were treated with GF (2.5 μM), ND (25 nM) or GF + ND for 24 hr. G2/M cell cycle arrest was measured by flow cytometry after exposure to drugs.

ing cell cycle in cells treated with either mock solution (Fig. 6a) or GF (40 μM , Fig. 6b) were then measured by flow cytometry analysis. As shown in Figure 6b, G2/M arrest was observed initially at 6 hr and reached the maximal level (>90%) at 24 hr after GF treatment. Similar results were also seen in COLO 205 cells (data not shown).

We then examined changes of G2/M regulatory proteins in HT 29 cells after GF treatment. Expression of cyclin B1/cdc2, a key regulator of cell entry into mitosis, was first monitored by immunoblotting and assaying the cyclin B1-immunoprecipitated cdc2 kinase activity. The time points according to Figure 6 were selected as 0 hr (representing the G0/G1 phase), 15 hr (representing the S phase), 18 hr (representing the G2/M phase) and 24 hr (representing the second G0/G1 phase). Immunoblotting analysis showed that cyclin B1 in mock-treated cells was elevated at 18 hr and then decreased at 24 hr (Fig. 7a). In the GF-treated group, the cyclin B1 levels accumulated initially at 15 hr and reached the maximal level at 24 hr. In addition, cdc2 kinase activity was elevated significantly in the GF-treated group although the change of protein level was not observed. The other G2/M regulatory protein, myt-1, which inhibits cdc2 kinase, was down-regulated in GF-treated cells.

It has been suggested that Bcl-2 phosphorylation is associated with G2/M cell cycle arrest.^{10,12,26,27} Figure 7a shows that the slower migration form of phosphorylated-Bcl-2 was present initially at 15 hr in cells treated with GF. The GF-induced phosphorylation changes of Bcl-2 were consistent with cells accumulating in the G2/M phase with an active cyclin B1/cdc2 complex. In this study, GF-mediated Bcl-2 phosphorylation coincided with cdc-2 kinase activation (Fig. 7a, lanes 6–8). Our results and those of others²⁷ indicate that cdc-2 kinase might be involved in Bcl-2 phosphorylation.

It has been shown that Bcl-2 may protect cancer cells from apoptosis.¹³ Human cancer cells exposed to paclitaxel expressed a phosphorylated form of Bcl-2 and underwent apoptosis, suggesting that phosphorylation of Bcl-2 may inhibit Bcl-2 function. In this study, we found that Bcl-2 phosphorylation appears to inhibit its binding to Bax, since less Bax was observed in an immunocomplex with Bcl-2 in GF-treated cancer cells (Fig. 7b). Our results demonstrate that Bcl-2 phosphorylation affects the binding ability

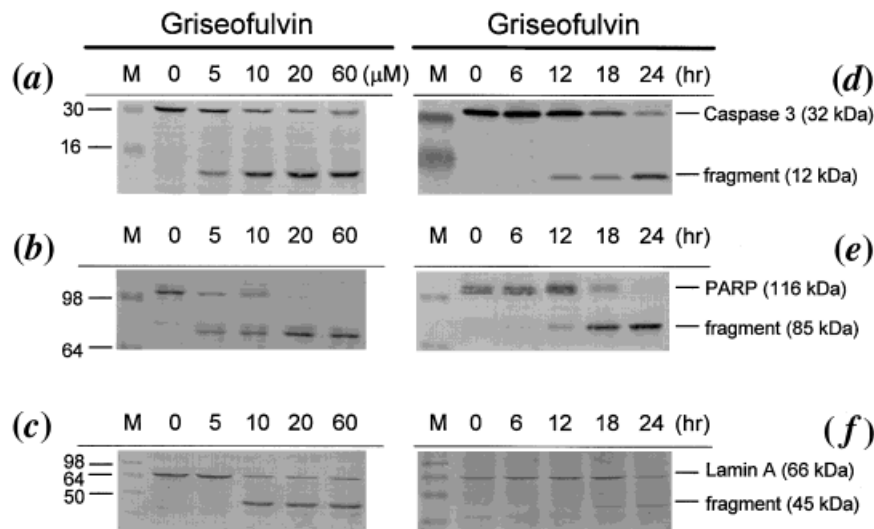


FIGURE 5 – Caspase-3 protein activation in griseofulvin (GF)-treated HT 29 cells undergoing apoptosis. (a, b, c) HT 29 cells were treated with various concentrations of GF (5–60 μM) for 24 hr. (d, e, f) HT 29 cells were treated with 10 μM of GF for the indicated time points. Proteins (50 μg /lane) were separated by sodium dodecyl sulfate-polyacrylamide gel electrophoresis, immunoblotted with caspase 3, poly-(ADP ribose) polymerase (PARP), or lamin A antibody and detected by the nitro blue tetrazolium/5-bromo-4-chloro-3-indolyl-phosphate (NBT/BCIP) system. Each blot is representative of 3 similar experiments.

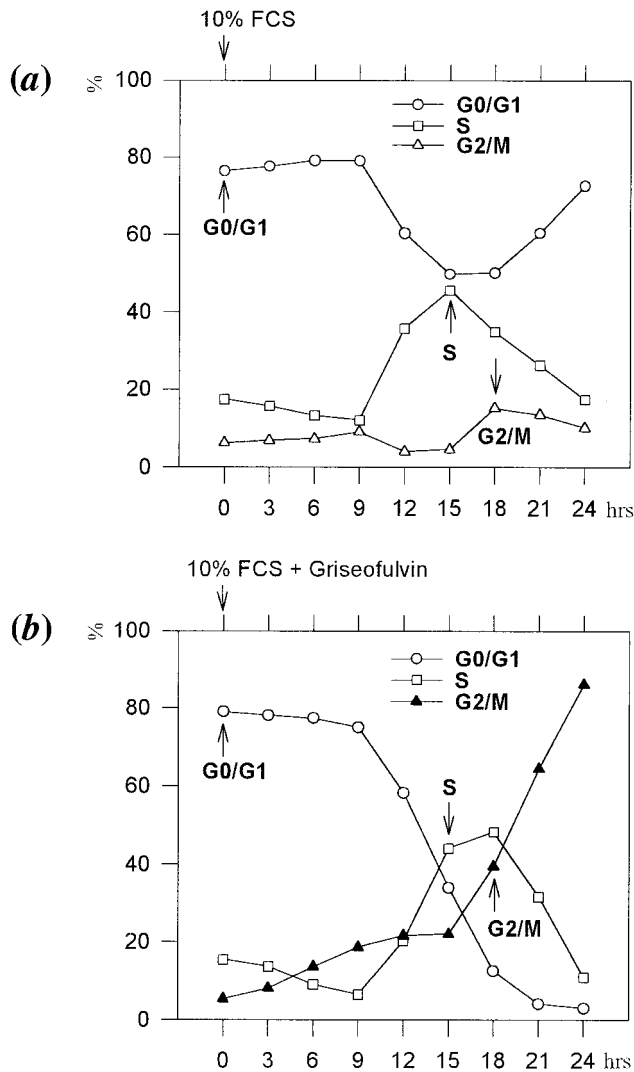


FIGURE 6 – Time-dependent response of griseofulvin (GF)-induced G2/M phase arrest in HT 29 cells. Cells were synchronized with 0.04% fetal calf serum (FCS) for 24 hr as described in Material and Methods. After synchronization, cells were then released into complete medium (10% FCS) containing (a) DMSO (0.1%), or (b) GF (40 μM). G2/M phase arrest was measured by flow cytometry at the indicated time points after exposure to GF.

to Bax and promotes abnormal microtubule polymerization, although the intracellular level of α -tubulin is not affected (Fig. 7b).

Combined treatment with GF and ND potentiates G2/M arrest in human cancer cells

Six types of human cells, including HT 29, COLO 205, Hep G2, Hep 3B, HL 60 and #76 KhGH, were used in this study. Cells were treated with various G2/M arrest-inducing agents including GF (20 μM), ND (0.25 μM), EP (20 μM) or combined treatment. Our results indicated that G2/M arrest after 24-h treatment with GF, EP and ND alone in HT 29 cells was 41%, 38.8% and 9.8%, respectively (Table I). Importantly, combined treatment with GF plus ND in HT 29 cells strongly potentiated the G2/M cell cycle arrest from 41% in GF and 9.8% in ND to more than 95.8% in combined treatment with both agents (Table I). Similar results were also observed in other cancer cell lines (Table I). In contrast, the potentiation of G2/M cell cycle arrest was not detected in normal human keratinocytes (#76 KhGH) (Table I). These results suggest

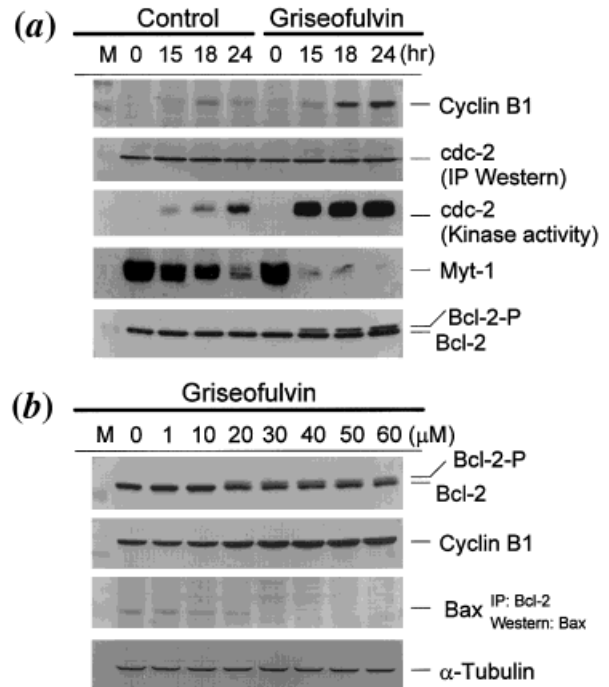


FIGURE 7 – Molecular mechanisms of G2/M arrest induced by griseofulvin (GF) in HT 29 cells. (a) HT 29 cells were synchronized with 0.04% fetal calf serum (FCS) for 24 hr as described in Material and Methods. After synchronization, cells were then released into complete medium (10% FCS) containing GF (20 μM) for 0, 15, 18 and 24 hr. HT 29 cells were also treated with DMSO (0.1%) as a control group. Proteins were loaded at 50 μg/lane. Protein extracts were separated by sodium dodecyl sulfate-polyacrylamide gel electrophoresis (SDS-PAGE), immunoblotted with anti-cyclin B1, myt-1, Bcl-2, or p34cdc2 antibody and detected by the NBT/BCIP system. The cyclin B1 antibody-immunoprecipitated p34cdc2 kinase activity from lysates of GF-treated HT 29 cells was also measured as described in Material and Methods. Each blot is representative of 3 similar experiments. (b) Dose-dependent response of GF-induced gene alterations in HT 29 cells. HT 29 cells were treated with various concentrations of GF (0–60 μM) for 24 hr. Protein extracts were separated by SDS-PAGE, immunoblotted with anti-cyclin B1, Bcl-2, or α -tubulin antibody and detected by the NBT/BCIP system. The Bcl-2 antibody-immunoprecipitated Bax protein from lysates of GF-treated HT 29 cells was also detected to investigate the ability of phosphorylated Bcl-2 to associate with Bax.

that G2/M arrest induced by a combination of GF and ND is specific to cancer cells.

To further scrutinize the underlying mechanisms of such observations, normal human keratinocytes (#76 KhGH) (Fig. 8, lanes 1–4) and HT 29 cells (Fig. 8, lanes 5–8) were subjected to a combined treatment with GF (20 μM) and ND (0.25 μM). As shown in Figure 8a (lane 8), phosphorylated Bcl-2 was significantly elevated in cells treated with a combination of both GF and ND. The protein level of cyclin B1/cdc2 and its kinase activity were also significantly elevated in HT 29 cells when treated with both GF and ND combined (Fig. 8, lane 8) as compared with the same treatment in normal keratinocytes (Fig. 8, lane 4). As shown in Figure 3, immunofluorescence staining of α -tubulin revealed that GF promotes tubulin polymerization. To further measure the ratio of tubulin polymerization, a simple assay was conducted by modifying a method originally described by Minotti *et al.*²⁰ The presence of GF and ND in the hypotonic buffer allowed the assay to be performed on a crude tubulin extract prepared from either HT 29 or #76 KhGH. We compared the relative ratios of soluble and polymerized tubulin prepared from HT 29 and #76 KhGH cells treated with GF (20 μM), ND (0.25 μM) or by combined treat-

TABLE I—SYNERGISTIC INDUCTION OF G2/M ARREST BY GF AND ND IN HUMAN CANCER CELLS

	HT 29			COLO 205			Hep G2			Hep 3B			HL 60			#76 KhGH		
	G0/G1	S	G2/M	G0/G1	S	G2/M	G0/G1	S	G2/M	G0/G1	S	G2/M	G0/G1	S	G2/M	G0/G1	S	G2/M
Control ¹	70.6	20.8	8.6	60.1	30.2	9.6	52.8	37.2	10.0	60.3	29.1	10.5	55.5	37.1	7.2	51.8	33.8	14.2
GF (20 μ M)	15.3	43.7	41.0	17.9	44.6	37.5	10.7	46.8	41.5	15.7	52.6	31.5	26.6	40.1	33.2	45.5	33.7	20.6
EP (20 μ M)	34.0	27.2	38.8	27.4	27.1	45.5	21.2	25.8	53.0	38.4	23.6	38.0	30.6	27.2	42.1	37.2	21.0	41.7
ND (0.25 μ M)	68.2	22.0	9.8	61.8	28.0	10.2	46.9	40.6	12.5	39.8	44.2	15.6	51.7	38.2	10.1	49.2	35.6	15.2
GF + EP	21.8	15.1	62.9	4.3	31.3	64.4	13.6	28.1	58.1	13.5	42.1	44.4	13.0	40.2	46.8	30.2	22.3	47.4
GF + ND	0.8	3.4	95.8	1.6	4.0	94.3	1.8	12.6	85.6	1.8	15.6	82.5	7.3	13.8	78.9	34.1	33.3	32.4

GF, griseofulvin; ND, nocodazole; EP, etoposide. Cells were treated with GF (20 μ M), EP (20 μ M), ND (0.25 μ M) or combination for 24 hr. After treatment, G2/M phase arrest was measured by flow cytometry as described in Materials and Methods.

¹Control cells were treated with DMSO (0.1%).

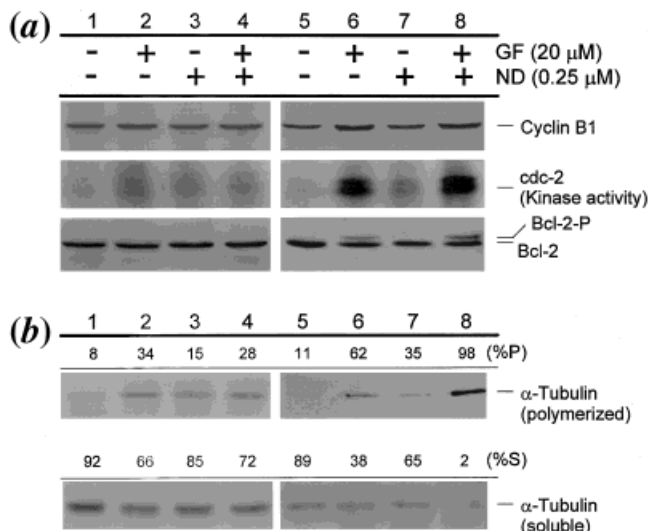


FIGURE 8—Molecular mechanisms of G2/M phase arrest by combined treatment of griseofulvin (GF) and nocodazole (ND). (a) Human normal keratinocytes (#76 KhGH) (lanes 1–4) and HT 29 cells (lanes 5–8) were subjected to GF (20 μ M), ND (0.25 μ M) or combined treatment for 24 hr. Cells were treated with DMSO (0.1%) as a control group. Proteins were loaded at 50 μ g/lane. Protein extracts were separated by sodium dodecyl sulfate-polyacrylamide gel electrophoresis, immunoblotted with anti-cyclin B1 or Bcl-2 antibody and detected by the NBT/BCIP system. The cyclin B1 antibody-immunoprecipitated cdc2 kinase activity from lysates of drug-treated cells was also measured as described in Material and Methods. Each blot is representative of 3 similar experiments. (b) *In vitro* tubulin polymerization assays by combined treatment of GF and ND in #76 KhGH and HT 29 cells. #76 KhGH (lanes 1–4) and HT 29 (lanes 5–8) cells were lysed with a hypotonic buffer, and the lysate were treated with either GF (20 μ M, lanes 2 and 6), ND (0.25 μ M, lanes 3 and 7), GF and ND (lanes 4 and 8) or without drugs (lanes 1 and 5) for 5 min at 37°C. The protein lysates containing polymerized (P) and soluble (S) fractions were then separated and probed with an antibody against α -tubulin as described in Material and Methods.

ment. In the absence of GF or ND, the majority of tubulin was found in the soluble form (Fig. 8b, lanes 1 and 5) and the ratios of polymerized and soluble tubulin were similar for both cell lines. In contrast, with combined treatment of GF and ND, tubulin polymerization was significantly elevated in HT 29 cells (Fig. 8b, lane 8) but not in #76 KhGH cells (Fig. 8b, lane 4). This *in vitro* system eliminated factors such as drug uptake and metabolism as experimental variables.

Treatment with GF and ND combination enhances cancer chemotherapeutic efficacy *in vivo*

We further examined the therapeutic efficacy of GF and ND *in vivo* by treating athymic mice bearing COLO 205 tumor xenografts with GF (50 mg/kg), ND (5 mg/kg) or GF and ND com-

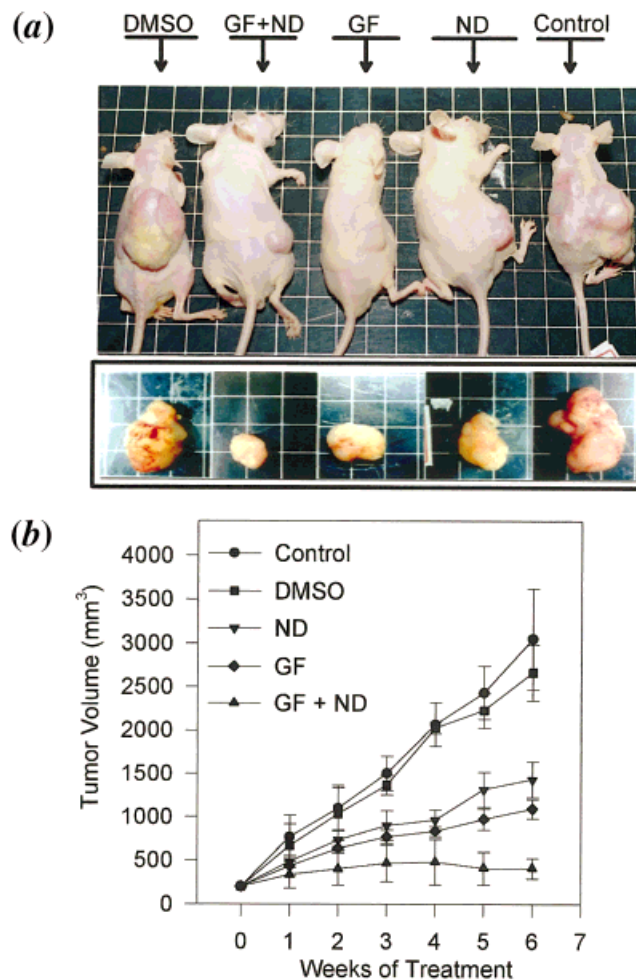


FIGURE 9—Griseofulvin (GF) enhances nocodazole (ND) efficacy in COLO 205 tumor xenografts. COLO 205 cells were injected subcutaneously between the scapulas of athymic mice. Once tumor volume reached approximately 200 mm³, the animal received intraperitoneal injection of GF (50 mg/kg), ND (5 mg/kg) or a combination of both agents 3 times per week. Vehicle (DMSO) or saline was also injected as a negative control. (a) The gross appearance of the mouse-bearing tumors was observed at 6 weeks after drug treatment. (b) Tumor volumes were measured weekly and estimated as described above.

bined. After establishment of palpable tumors (mean tumor volume, 200 mm³), animal received intraperitoneal injections of GF, ND or both agents together 3 times per week, as well as DMSO and saline for a negative control. After 6 weeks, tumor volumes in mice treated with either GF or ND were significantly less in comparison with those in DMSO- or saline-treated controls (Fig. 9). Treatment with GF and ND together significantly enhanced the

efficacy of ND, leading to cessation of tumor growth (Fig. 9a,b). In mice receiving these treatment regimens, no gross signs of toxicity were observed (body weight, visible inspection of general appearance and microscopic examination of individual organs). Our results provide further evidence that GF may have significance of application for cancer chemotherapeutic purposes.

DISCUSSION

GF activated signaling pathways that trigger both G2/M arrest and apoptosis

Previous studies have demonstrated that various cancer chemotherapeutic agents targeting microtubule can lead to apoptosis *in vitro*⁸ and *in vivo*.²⁸ In this study, we demonstrated that GF-promoted abnormal microtubule stabilization similarly initiates a cascade of events leading to apoptosis. Our results demonstrated that initiation of apoptosis was observed more rapidly with GF (12–24 hr) as compared with effective doses of ND, paclitaxel and other microtubule-damaging agents (24–72 hr).^{8,12} In this study, a dose-dependent experiment was performed and demonstrated that a lower dose of GF (10 μ M) induced apoptosis in HT 29 cells, whereas higher doses of GF (>20 μ M) initiated significant G2/M arrest (Figs. 2 and 3). Higher doses of GF (>20 μ M) cause an increase of cell death and G2/M mitotic arrest, which appears to be unrelated to apoptosis. Our results support the hypothesis that GF activated some signaling pathways, which trigger both G2/M arrest and apoptosis with a lower threshold of apoptosis. Recent studies^{8,29} have suggested that paclitaxel-induced apoptosis may occur via a signaling pathway independent of microtubule and mitotic arrest. Although it has been well recognized that anti-microtubule agents can cause both mitotic arrest and apoptotic cell death, it remains unclear whether apoptosis induced by these agents is a secondary event resulting from mitotic arrest or represents a novel mechanism of action for these antimicrotubule agents against tumor cells.

Combined treatment with GF and ND is significant for application for cancer chemotherapeutic purposes

In normal cells, the dynamic instability of microtubules is thought to be critically important to normal microtubule functions, including mitosis.³⁰ Unusual stabilization of mitotic spindles is thought to be a common mechanism of microtubule poisons such as paclitaxel.³¹ Previous studies indicated that the primary intracellular action of paclitaxel is to specifically bind to cytoplasmic microtubules in a reversible manner.³² Another study,³³ however, demonstrated that paclitaxel-induced apoptosis is an irreversible process, which contrasts with the reversible manner of paclitaxel binding to microtubules. Recently, various cancer chemotherapeutic agents, which block apoptosis through unusual stabilization of microtubules, simultaneously initiated a cascade of events leading to apoptosis.^{8,9} Another study³⁴ indicated that the toxicity of ND was specific for cells from human but not from mouse and hamster. These data suggest that there is a species-specific cytoskeletal damage response pathway. However, the toxicity induced by these cancer chemotherapeutic agents has been observed frequently, including neutropenia, myalgias, mucositis, neuropathies and alopecia.³⁵ To minimize the toxicity in normal human cells and promote the specificity of anti-neoplastic effects in cancer cells, low dose of ND was used in combination with GF. Our study demonstrated that synergistic induction of apoptosis and G2/M arrest occurs only in human cancer cells. Combined treatment of

both GF and ND in athymic mice bearing human colorectal cancer xenografts also revealed the consistent results observed *in vitro*.

P34 cdc2 kinase activation and Bcl-2 phosphorylation

Some studies^{10,36,37} have demonstrated that anti-microtubule agents induce phosphorylation of Bcl-2 protein, whereas DNA-damaging agents do not. Our results extend these previous findings and demonstrate that G2/M mitotic arrest and apoptosis were enhanced synergistically in cells by combined treatment of GF and ND. Our results show that the mechanisms of G2/M cell cycle arrest include cyclin B/cdc2 kinase activation, Bcl-2 phosphorylation and abnormal tubulin polymerization. Significant phosphorylation of Bcl-2 was observed in HT 29 cells treated with ND and GF in which cyclinB/cdc2 kinase activity was consistently activated (Fig. 8). We do not exclude the possibility that some other kinase(s) might be also involved in the phosphorylation of Bcl-2, and might be more easily induced in human cancer cells than in normal keratinocytes.

Several kinases, including c-jun N-terminal kinase,³⁸ Raf-1,^{37,39} PKA¹⁰ and the cyclinB1/cdc2 complex,^{13,36} have been suggested to be involved in Bcl-2 phosphorylation. From the results, we predict that the kinase involved in GF-mediated Bcl-2 phosphorylation is part of the mitotic kinase cascade activated by p34cdc2. It has been demonstrated previously that Bcl-2 is phosphorylated on the 17 serine residues, and several serine residues could be potential sites of phosphorylation by different kinases.^{37,38} It is not yet known whether the same sites are hyperphosphorylated by microtubule-damaging drugs. Further studies are needed to identify the site(s) of hyperphosphorylation in Bcl-2 protein by these drugs and to define the relevant kinases. As previously reported, paclitaxel activates p34cdc2 kinase activity, which in turn causes apoptosis.¹¹ The induction of apoptosis in GF-treated tumor cells has been proposed to result from activation of p34cdc2, which in turn causes hyperphosphorylation of Bcl-2 and then inhibits its ability to heterodimerize with Bax and eventually induce apoptosis.

Possible mechanisms of GF-induced G2/M arrest and apoptosis

As described above, the G2/M arrest and apoptosis effects were initiated by GF through some signaling pathways with lower threshold for apoptosis. Based on the phenomena discussed above and the well-known cellular action of GF on mitotic arrest, we hypothesize two possible pathways by which GF could cause cell death. The first pathway could be considered as the microtubule pathway, by which cell death occurs following mitotic arrest at higher dose of GF (>20 μ M) treatment. Briefly, after GF crosses the plasma membrane, it binds specifically to cytoplasmic microtubules and promotes the formation of unusually stable microtubules. The stabilization effect leads to cell cycle arrest at the G2/M phase. Eventually, cells arrested at the G2/M phase may die by apoptosis. In this case, apoptotic cell death is considered as a secondary event resulting from mitotic arrest. The second pathway assumes that GF exerts its cell-killing activity through a gene-directed process, such as caspase(s) activation, in cells under a low-dose GF (10 μ M) treatment. The activation of caspase 3 could be consequence of the cell death process rather than causal. Further investigation must be performed to illustrate the role of other caspase(s) signaling pathways in GF-induced apoptosis. However, these two pathways could occur simultaneously, as in our demonstration that higher dose of GF treatment induces both apoptosis and G2/M arrest.

REFERENCES

- Boise LH, Gonzalez-Garcia M, Postema CE, Ding L, Lindsten T, Turka LA, et al. Defining apoptosis. *Am J Pathol* 1995;146:16–9.
- Boise LH, Gonzalez-Garcia M, Postema CE, Ding L, Lindsten T, Turka LA, et al. Bcl-x, a Bcl-2 related gene that function as a dominant regulator of apoptotic cell death. *Cell* 1993;74:597–608.
- Reed JC. Bcl-2 and the regulation of programmed cell death. *J Cell Biol* 1994;124:1–6.
- Kroemer G. The proto-oncogene Bcl-2 and its role in regulating apoptosis. *Nat Med* 1997;3:614–20.
- Pieten JA, Papadopoulos N, Markowitz S, Willson JKV, Kinzler KW, Vogelstein B. Paradoxical inhibition of solid tumor cell growth by Bcl-2. *Cancer Res* 1994;54:3714–7.
- Oltvai ZN, Milliman CL, Korsmeyer SJ. Bcl-2 heterodimerizes *in vivo* with a conserved homolog, Bax, that accelerates programmed cell death. *Cell* 1993;74:609–19.
- Michael F, Christel H, Gerhard B. Induction of nuclear accumulation of the tumor-suppressor protein p53 by DNA damaging agents. *Oncogene* 1993;8:307–18.

8. Jordan MA, Wendell K, Gardiner S, Derry WB, Copp H, Wilson L. Mitotic block induced in HeLa cells by low concentrations of paclitaxel (taxel) results in abnormal mitotic exit and apoptotic cell death. *Cancer Res* 1996;56:812–25.
9. Mooberry SL, Busquets L, Georgia T. Induction of apoptosis by cryptophycin 1, a new antimicrotubule agent. *Int J Cancer* 1997;73:440–8.
10. Srivastava RK, Srivastava AR, Korsmeyer SJ, Nesterova M, Cho-Chung YS, Longo DL. Involvement of microtubules in the regulation of Bcl-2 phosphorylation and apoptosis through cyclic AMP-dependent protein kinase. *Mol Cell Biol* 1998;18:3509–17.
11. Donaldson KL, Goolsby GL, Kiener PA, Wahl AF. Activation of p34cdc2 coincident with taxol-induced apoptosis. *Cell Growth Differ* 1994;5:1041–50.
12. Haldar S, Chintapalli J, Croce CM. Taxol induces Bcl-2 phosphorylation and death of prostate cancer cells. *Cancer Res* 1996;56:1253–5.
13. Haldar S, Basu A, Croce CM. Bcl-2 is the guardian of microtubule integrity. *Cancer Res* 1997;57:229–33.
14. Ling YH, Tornos G, Perez-Soler R. Phosphorylation of Bcl-2 is a marker of M phase events and not a determinant of apoptosis. *J Biol Chem* 1998;273:18984–91.
15. Roth W, Wagenknecht B, Grimm C, Dichgans J, Weller M. Taxol-mediated augmentation of CD95 ligand-induced apoptosis of human malignant glioma cells: association with Bcl-2 phosphorylation but neither activation of p53 nor G2/M cell cycle arrest. *Br J Cancer* 1998;77:404–11.
16. Poruchynsky MS, Wang EE, Rudin CM, Blagosklonny MV, Fojo T. Bcl-xL is phosphorylated in malignant cells following microtubule disruption. *Cancer Res* 1998;58:3331–8.
17. Ho YS, Tsai PW, Yu CF, Liu HL, Chen RJ, Lin JK. Ketoconazole induced apoptosis through p53-dependent pathway in human colorectal and hepatocellular carcinoma cell lines. *Toxicol Appl Pharmacol* 1998;15:39–47.
18. Ho YS, Lee HM, Chang CR, Lin JK. Induction of Bax protein and degradation of lamin A during the p53-dependent apoptosis induced by chemotherapeutic agents in human cancer cell lines. *Biochem Pharmacol* 1999;57:143–54.
19. Ho YS, Lee HM, Mou TC, Wang YJ, Lin JK. Suppression of nitric oxide induced apoptosis by L-N-acetyl-cysteine through modulation levels of glutathione, Bcl-2 and Bax proteins. *Mol Carcinogen* 1997;19:101–13.
20. Minotti AM, Barlow SB, Cabral F. Resistance to antimetabolic drugs in Chinese hamster ovary cells correlates with changes in the level of polymerized tubulin. *J Biol Chem* 1991;266:3987–94.
21. Ho YS, Wang YJ, Lin JK. Induction of p53 and p21/WAF1/CIP1 expression by nitric oxide and their association with apoptosis in human cancer cells. *Mol Carcinogen* 1996;16:20–31.
22. Oki E, Sakaguchi Y, Toh Y, Oda S, Maehara Y, Yamamoto N, et al. Induction of apoptosis in human tumor xenografts after oral administration of uracil and tegafur to nude mice bearing tumors. *Br J Cancer* 1998;78:625–30.
23. Enari M, Sakahira H, Yokoyama H, Okawa K, Iwamoto A, Nagata S. A. Caspase-activated DNase that degrades DNA during apoptosis, and its inhibitor ICAD. *Nature* 1998;391:43–50.
24. Alnemri ES, Livingston DJ, Nicholson DW, Salvesen G, Thornberry NA, Wong WW, et al. Human ICE/CED-3 protease nomenclature. *Cell* 1996;87:171.
25. Nicholson DW, Ali A, Thornberry NA, Vaillancourt JP, Ding CK, Gallant M, et al. Identification and inhibition of the ICE/CED-3 protease necessary for mammalian apoptosis. *Nature (Lond)* 1995;376:37–43.
26. Scatena CD, Stewart ZA, Mays D, Tang LJ, Keefer CJ, Leach SD, et al. Mitotic phosphorylation of Bcl-2 during normal cell cycle progression and taxol-induced growth arrest. *J Biol Chem* 1998;273:30777–84.
27. Stewart ZA, Mays D, Pietsenpol JA. Defective G1-S cell cycle checkpoint function sensitizes cells to microtubule inhibitor-induced apoptosis. *Cancer Res* 1999;59:3831–7.
28. Milas L, Hunter NR, Kurdoglu B, Mason KA, Meyn RE, Stephens LC, et al. Kinetics of mitotic arrest and apoptosis in murine mammary and ovarian tumors treated with taxol. *Cancer Chemother Pharmacol* 1995;35:297–303.
29. Lieu CH, Chang YN, Lai YK. Dual cytotoxic mechanisms of submicromolar taxol on human leukemia HL-60 cells. *Biochem Pharmacol* 1997;53:1587–96.
30. Mitchison TJ, Kirschner M. Dynamic instability of microtubule growth. *Nature (Lond)* 1984;312:237–42.
31. Wani MC, Taylor HL, Wall ME, Coggon P, McPhail AT. Plant antitumor agents. VI. The isolation and structure of taxol, a novel antileukemic and antitumor agent for *Taxus brevifolia*. *J Am Chem Soc* 1971;93:2325–7.
32. Parekh HK, Simpkin H. Species-specific differences in taxol transport and cytotoxicity against human and rodent tumor cells. Evidence for an alternate transport system? *Biochem Pharmacol* 1996;51:301–11.
33. Cheng L, Zheng S, Raghunathan K, Priest DG, Willingham MC, Norris JS, et al. Characterization of paclitaxel-induced apoptosis and altered gene expression in human breast cancer cells. *Cell Pharmacol* 1995;2:249–57.
34. Gupta RS. Species-specific differences in toxicity of antimetabolic agents toward cultured mammalian cells. *J Natl Cancer Inst* 1985;74:159–64.
35. Guchelaar HJ, Ten Napel CH, De Vries EG, Mulder NH. Clinical, toxicological and pharmaceutical aspects of the antineoplastic drug taxol: a review. *Clin Oncol* 1994;6:40–8.
36. Haldar S, Jena N, Croce CM. Inactivation of Bcl-2 by phosphorylation. *Proc Natl Acad Sci U S A* 1995;92:4507–11.
37. Blagosklonny MV, Giannakakou P, Ei-Deiry WS, Kingston DGI, Higgs PI, Neckers L, et al. Raf-1/Bcl-2 phosphorylation: a step from microtubule damage to cell death. *Cancer Res* 1997;57:130–5.
38. Maudrell K, Antonsson B, Magnenat E, Camps M, Muda M, Chabert C, et al. Bcl-2 undergoes phosphorylation by c-Jun-N-terminal kinase/stress-activated protein kinases in the presence of the constitutively active GTP-binding protein Rac1. *J Biol Chem* 1997;272:25238–42.
39. Blagosklonny MV, Schulte T, Nguyen P, Trepel J, Neckers LM. Taxol-induced apoptosis and phosphorylation of Bcl-2 protein involves c-Raf-1 and represents a novel c-Raf-1 signal transduction pathway. *Cancer Res* 1996;56:1851–4.